Fault Location in Power Distribution System With Penetration of Distributed Generation

Sukumar M. Brahma, *Senior Member, IEEE*

***Abstract*—It has been shown that coordination between protective devices in distribution systems in the presence of significant distributed generation (DG) will be disrupted. With the recent trend of adopting and integrating renewable resources and microgrids with distribution systems, it is probable that distribution systems will have significant and arbitrary penetration of DG in the near future. This will change the distribution systems to multisource unbalanced systems where protective devices may not coordinate. The fault location in this type of system will be a challenge. This paper describes a general method to locate faults in this type of system. The method uses synchronized voltage and current measurements at the interconnection of DG units and is able to adapt to changes in the topology of the system. The method has been extensively tested on a 60-bus distribution system for all types of faults with various fault resistances on all sections of the system, with very encouraging results.**

***Index Terms*—Bus impedance matrix, distributed generation (DG), fault, power distribution system, power system protection.**

I. Introduction

TYPICALLY, a distribution feeder, as shown in Fig. 1, originates from a substation at voltages usually less than 35 kV and consists of a main feeder and tapped laterals. A distribution system is formed by several of these feeders originating at the substation. The system is unbalanced in terms of load, phases, and line impedances. The nature of traditional distribution systems is single sourced and radial with the substation source feeding a series of downstream feeders.

This nature of traditional distribution systems is undergoing a change due to the penetration of distributed generation (DG). With the increased cost of transmission and distribution, renewed interest and substantial investment in renewable technologies, the requirement of the utilities in most states in the U.S. for renewable portfolios and potential evolution of microgrids connecting to the main distribution feeders has contributed to the possibility of very rapid growth of DG getting connected directly to distribution systems [1], [2]. DG is defined as the generation ranging from a few kilowatts to a few megawatts (micro to large) and typically interconnected at substation, distribution feeder, or customer load level [3]. DG technologies include photovoltaic, wind turbines, fuel cells, micro turbines, gas turbines, and internal combustion engines among other alternatives [3]. In recent times, microgrid is a topic of intense research [4] and the entire microgrid can connect to a distribution feeder acting as an aggregated load and source. These changes mean that the nature of the distribution system will change to a multisource unbalanced system. It is almost certain that the distribution system of the near future will depend on DG for continuous load support, not just for peak load shaving. Moreover, the penetration of DG is most likely to be arbitrary and the utility may not have adequate control over the number and placement of DG units connected to their distribution systems.

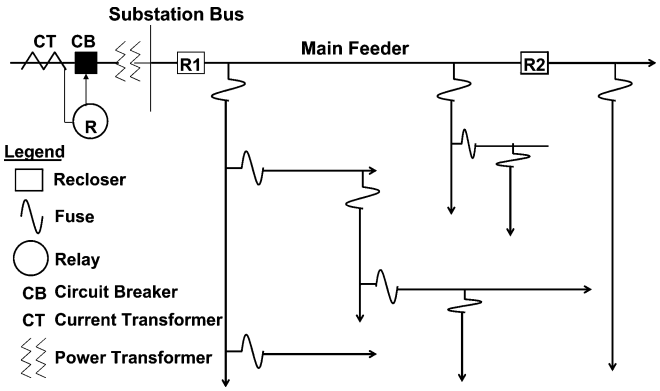

Fig. 1. Traditional distribution system.

Fault location in a distribution system has two aspects: the first is to identify and isolate the faulted section and the second is to locate the fault exactly on the faulted section. Traditionally, the first aspect is accomplished by the protection system. The main protective devices used in a distribution system are fuses, reclosers, and relays as shown in Fig. 1. A protection system is comprised of a combination of these devices coordinated in a way that ensures correct identification and isolation of the faulted section. In a traditional distribution system, the protection system is designed with the assumption that the system is single source and radial [5], [6]. The fault-location methods for these distribution systems also make the same assumption. Since the system with DG is no longer single source, the underlying assumptions for both of these aspects of fault location break down. In order to address fault location in distribution systems with DG, both of these aspects need to be re-evaluated in the presence of DG and any new scheme should reconcile with this evaluation.

Hadjsaid *et al.* [7] show through simple examples that fault currents through protective devices would change after the introduction of DG. This paper further suggests checking protection selectivity when each new DG unit is connected. However, this solution would work only if DG penetration is low. Brahma and Girgis [8], [9] look closely at the coordination problem between fuses. They observe that for a given fault, fault currents

Manuscript received March 29, 2010; revised October 28, 2010; accepted January 06, 2011. Date of publication February 24, 2011; date of current version June 24, 2011. This work was supported by the Energy Innovation Small Grants (EISG) Program of the California Energy Commission. Paper no. TPWRD-00231-2010.

The author is with the Klipsch School of Electrical and Computer Engineering, New Mexico State University, Las Cruces, NM 88003 USA (e-mail: sbrahma@nmsu.edu).

Digital Object Identifier 10.1109/TPWRD.2011.2106146

may flow downstream as well as upstream in the faulted section. Reference [9] considers scenarios with different capacities, number, and location of DG units in a system protected by fuses. This paper concludes that, in general, if the protection scheme is not changed, the only way to maintain coordination in the presence of arbitrary DG penetration is to disconnect all DG units instantaneously in case of a fault. This would enable the system to regain its radial nature and coordination would withhold. But this would mean that DG is disconnected even for temporary faults.

Brahma and Girgis [8], [10] discuss fuse-recloser coordination in the presence of DG. They show that different currents can flow through the coordinated fuse and recloser for a given fault. Since these devices are coordinated for the same fault current flowing through them, the coordination can be lost. Moreover, fault current will flow through the recloser even for upstream faults due to the presence of DG. Reference [10] discusses this situation in detail and concludes that coordination in the presence of DG can be achieved with microprocessor-based reclosers available in the market. However, in this case too, all DG units downstream of the recloser would have to be disconnected before the first reclose takes place to avoid connection of two live subsystems without synchronism. Thus, in this case too, DG has to be disconnected for all temporary faults. Reference [11] shows that even this coordination is likely to malfunction in the presence of significant fault resistance. References [12] and [13] mention some case-specific coordination issues involving fuses, reclosers, and relays.

The solutions mentioned before are impractical. As mentioned earlier, the future distribution systems will depend on DG for continuous load support, at least when DG penetration is substantial. Disconnecting all DG units for all temporary faults would make the system very unreliable, especially because the majority of the faults taking place in a distribution system are temporary [6], [14]. Thus, the present protection scheme is inadequate to coordinate meaningfully in the presence of significant DG.

There is some published literature on fault location in distribution systems in the presence of DG. Lu *et al.* [15], Xiangjun *et al.* [16], and Javadian *et al.* [17] present fault-location techniques for primary distribution feeders in the presence of DG. These methods assume radial sections being controlled by relays and circuit breakers. These methods will not translate to laterals protected by fuses. El-Fouly *et al.* [18] and Marvik *et al.* [19] discuss the issues that may arise in fault location in distribution systems due to the penetration of DG. The papers do not provide any clear solutions. Guo-fang and Yu-ping [20], [21] present fault-location schemes applicable to distribution systems where DG units are connected only at the ends of laterals. This topology is very restrictive. Javadian *et al.* [22] present a scheme using multilayer perceptrons (MLP) that recommends the system be broken into radial zones, each zone being protected by a circuit breaker. This needs extensive modification to the system topology. Calderaro *et al.* [23] present a scheme using Petri nets that needs current direction in different sections as the input. A large number of sensors are required to localize the fault to a reasonably small zone. The exact fault location is not attempted. Chao *et al.* [24] present a method based on graph theory, but do not perform the exact fault location. Their simulations are not rigorous enough to even support their claim of correct section identification. Bretas and Salim [25] present a scheme based on positive-sequence apparent impedance. Their modeling is very simplistic, as they ignore the inherent unbalance in distribution systems and even ignore mutual coupling between phases. Johnsonbough and Girgis [26] describe a method which is a modification of the apparent impedance method described in [27]. However, the work fails to capture the realistic multilateral multisource nature of the system and reports unacceptably large errors in many cases. Brahma and Girgis [28] develop a scheme to locate the faulted section following a superposition-based approach and using precalculated short-circuit results. However, the work does not locate the fault exactly on the faulted section and the use of the precalculated short circuit results is a source of error. None of the methods listed above try to capture the effect of fault resistance. Thus, the problem of fault location in distribution systems with DG still remains to be solved comprehensively, especially for fused laterals and secondary distribution networks.

The following issues emerge from the above discussion:

1) The fault location scheme cannot assume that the faulted section is known accurately, because the protective devices could have lost coordination and the wrong device /devices may have operated.
2) There is a need for a fault location method that considers the multi-source unbalanced nature of the distribution system with DG.

This paper presents a generalized method to resolve these issues. Section II shows the theoretical formulation of the method. Section III describes the simulation results from applying the methodology to a 60-bus distribution system. Section IV presents concluding remarks.

II. Formulation of the Methodology

A. Thevenin Models of DG

The proposed method will use the positive-, negative-, and zero-sequence Thevenin equivalents of each type of source as shown in Fig. 2 with conventional notations. Barker *et al.* [29] provide a range of Thevenin impedances for inverters, synchronous generators, and induction generators. However, the exact values are provided in the manufacturer's manual for specific DG units. The methodology adopted in this paper uses a simple method based on voltage and current measurements at the connection of DG unit to determine the Thevenin impedance. This method is now illustrated.

Equations for this method are derived assuming that DG units inject only positive-sequence voltages and currents into the system under load conditions. However, they can be easily modified to include negative- or zero-sequence injections if the case demands. The notations used for the prefault values of $V^{(1)}$ and $I^{(1)}$ are V_L and I_L, respectively, and those for the positive-sequence fault values are $V_F^{(1)}$ and $I_F^{(1)}$, respectively. The equation describing the prefault condition is

$$E = V_L + Z_S^{(1)} I_L. \tag{1}$$

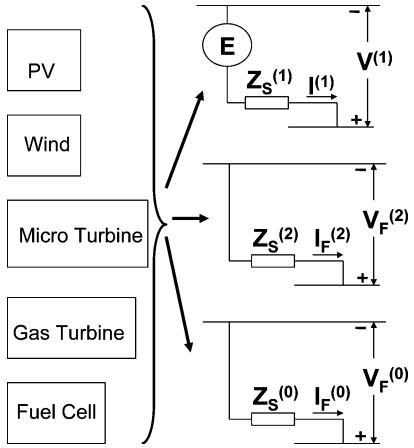

Fig. 2. Thevenin equivalent of DG.

The equation describing the fault condition is

$$E = V_F^{(1)} + Z_S^{(1)} I_F^{(1)}. \tag{2}$$

Subtracting (2) from (1), we obtain

$$V_L - V_F^{(1)} = Z_S^{(1)} \left(I_F^{(1)} - I_L \right). \tag{3}$$

$V_L - V_F^{(1)}$ and $I_F^{(1)} - I_L$ are changes, respectively, in positive-sequence bus voltage and positive-sequence bus current due to fault. Denoting these changes by $\Delta V^{(1)}$ and $\Delta I^{(1)}$, (3) can be rewritten as

$$Z_S^{(1)} = \frac{\Delta V^{(1)}}{\Delta I^{(1)}}. \tag{4}$$

Similarly, the negative-sequence and the zero-sequence Thevenin impedances can be found by using

$$Z_S^{(2)} = -\frac{V_F^{(2)}}{I_F^{(2)}} \tag{5}$$

$$Z_S^{(0)} = -\frac{V_F^{(0)}}{I_F^{(0)}}. \tag{6}$$

The values of voltages and currents during normal and faulted operations can be obtained from the measuring devices located at the output terminals of the DG unit. These voltages and currents can be resolved into sequence components and the sequence impedances can be calculated by using (4)–(6). Once the Thevenin equivalent sequence impedances are known, they can be converted to the coupled phase impedance matrix Z_{abc} by using (7) [30]

$$\begin{aligned} Z_{abc} &= \begin{bmatrix} Z_{Sa} & Z_{Sab} & Z_{Sac} \\ Z_{Sba} & Z_{Sb} & Z_{Sbc} \\ Z_{Sca} & Z_{Scb} & Z_{Sc} \end{bmatrix} \\ &= \frac{1}{3} \begin{bmatrix} 1 & 1 & 1 \\ 1 & a & a^2 \\ 1 & a^2 & a \end{bmatrix} \begin{bmatrix} Z_S^{(0)} & 0 & 0 \\ 0 & Z_S^{(1)} & 0 \\ 0 & 0 & Z_S^{(2)} \end{bmatrix} \\ &\quad \times \begin{bmatrix} 1 & 1 & 1 \\ 1 & a^2 & a \\ 1 & a & a^2 \end{bmatrix} \end{aligned} \tag{7}$$

where $a = e^{j2\pi/3}$.

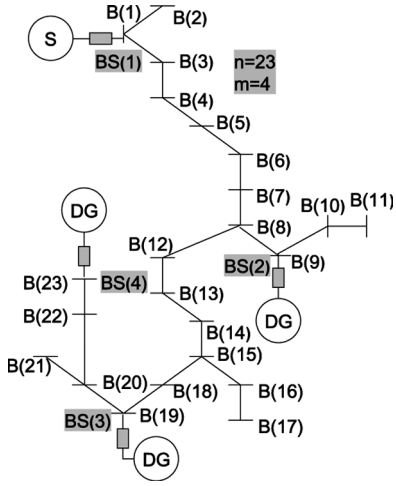

Fig. 3. Single-line diagram of the example system.

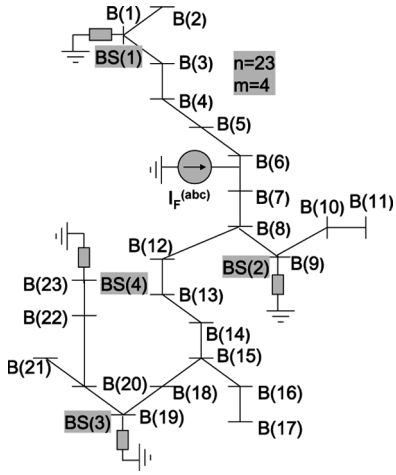

Fig. 4. Network equivalent of the faulted system.

With the three-phase source impedances known, the three-phase bus impedance matrix $Z_{\text{bus}}^{(abc)}$ of the distribution system can be determined [31]. $Z_{\text{bus}}^{(abc)}$ can accurately model all system unbalances [31], [32] and will be used by the proposed fault-location scheme described in Section II-B. The advantage of this approach is that the correct source impedance will be measured and modeled into the bus impedance matrix irrespective of the type of the DG unit, or its interface.

B. Fault-Location Scheme

The intent of this scheme is to locate the fault without depending on the protective devices to correctly identify the faulted section. The proposed scheme assumes that digital fault recorders (DFRs) are located at the substation source and at the connection point of each DG and they record voltages and currents of all three phases. Moreover, the scheme assumes that the waveforms obtained from all DFRs are available as synchronized phasors. These assumptions are well within the present practices and the present state of technology [33]. The scheme also assumes that $Z_{\text{bus}}^{(abc)}$ of the distribution system is known, as explained in Section II-A. The proposed method will be explained through the example distribution system shown as a one-line diagram in Fig. 3 and its fault-time equivalent network shown in Fig. 4. The

current injection $I_F^{(abc)}$ models the fault, with or without fault resistance. Its location can be anywhere in the system.

The first part of this scheme identifies the faulted section without depending on the operation of any protective device. Let us assume the total number of buses in the system to be n and the total number of sources in the system (including the substation source) to be m. The sources are denoted by $S1, S2, \ldots Sm$. The buses are denoted by $B(1), B(2), \ldots B(n)$. The buses to which these sources are connected are denoted by $BS(1), BS(2), \ldots BS(m)$. In a three-phase model of the system, the $Z_{\text{bus}}^{(abc)}$ will be $3n \times 3n$ matrix and the voltages and currents would be 3×1 vectors. Adjustments can be made to include one-phase and two-phase lines and buses [31], [32]. For the faulted condition, the change in the three-phase voltages at bus I due to a fault at bus J is given by (8) for the three-phase model of the system [31]

$$\Delta V_{I-J}^{(abc)} = Z_{bus}^{(abc)}(I, J) \times I_F^{(abc)}. \tag{8}$$

The superscript (abc) in (8) and in the rest of this document denotes the three-phase equivalents of the respective elements. $I_F^{(abc)}$ is the three-phase fault current injection at bus J. $\Delta V_{I-J}^{(abc)}$ denotes the change in the three-phase voltage values at bus I due to the injected current $I_F^{(abc)}$ at bus J. Since it is assumed that synchronized phasors of all three-phase voltages and currents are available at all sources, the total fault current can be calculated by summing the fault current contributions from all sources. Thus, $I_F^{(abc)}$ in (8) is known. Moreover, from the elements of the vector $I_F^{(abc)}$, the type of fault and the faulted phases can also be known if needed.

The fault-location algorithm starts by assuming that the fault is located on bus $B(1)$. Using (8), the algorithm calculates the change in the three-phase voltages at all source buses in the system $\left(\Delta V_{BS(j)-B(1)}^{(abc)},\ j = 1, 2 \ldots m\right)$ for the assumed fault location. The actual change in bus voltages is already available at buses $BS(1), BS(2), \ldots BS(m)$ from the measurement of the prefault and the fault voltages. Let us denote these by $\Delta V_{BS(j)-obs}^{(abc)},\ j = 1, 2, \ldots m$. The following error index is created:

$$\text{Error}(1) = \sum_{j=1}^{m} norm\left(\Delta V_{BS(j)-B(1)}^{(abc)} - \Delta V_{BS(j)-obs}^{(abc)}\right) \tag{9}$$

where the norm for a $k \times 1$ vector X is defined as

$$\text{norm}(X) = \left[|X(1)|^2 + |X(2)|^2 + |X(3)|^2 + \cdots |X(k)|^2\right]^{1/2}. \tag{10}$$

While applying (10) to (9), the vector $\Delta V_{BS(j)-B(1)}^{(abc)} - \Delta V_{BS(j)-obs}^{(abc)}$ is 3×1 (i.e., $k = 3$). The algorithm will then assume the fault to be at $B(2), B(3), \ldots B(n)$ and for each case generate error indices $Error(1), Error(2), \ldots Error(n)$, respectively, using (9).

To understand this process more clearly, let us assume the system in Fig. 3 has a fault. The total fault current can be calculated by summing the three-phase current injections at buses $BS(1)$, $BS(2)$, $BS(3)$, and $BS(4)$, which are the same as $B(1)$, $B(9)$, $B(19)$, and $B(23)$, respectively. Using this fault current vector and (8), $\Delta V_{BS(1)-B(1)}^{(abc)}$, $\Delta V_{BS(2)-B(1)}^{(abc)}$, $\Delta V_{BS(3)-B(1)}^{(abc)}$, and $\Delta V_{BS(4)-B(1)}^{(abc)}$ can be calculated, assuming the fault is on bus $B(1)$. The observed values of the change of voltages at the source buses due to fault are denoted by $\Delta V_{BS(1)-obs}^{(abc)}$, $\Delta V_{BS(2)-obs}^{(abc)}$, $\Delta V_{BS(3)-obs}^{(abc)}$, and $\Delta V_{BS(4)-obs}^{(abc)}$. The error in this case would be

$$\begin{aligned}\text{Error}(1) &= norm\left(\Delta V_{BS(1)-B(1)}^{(abc)} - \Delta V_{BS(1)-obs}^{(abc)}\right) \\ &+ norm\left(\Delta V_{BS(2)-B(1)}^{(abc)} - \Delta V_{BS(2)-obs}^{(abc)}\right) \\ &+ norm\left(\Delta V_{BS(3)-B(1)}^{(abc)} - \Delta V_{BS(3)-obs}^{(abc)}\right) \\ &+ norm\left(\Delta V_{BS(4)-B(1)}^{(abc)} - \Delta V_{BS(4)-obs}^{(abc)}\right). \end{aligned} \tag{11}$$

The algorithm would then proceed to assume the fault to be at bus $B(2), B(3), \ldots B(23)$ and generate $\text{error}(2), \text{error}(3), \ldots \text{error}(23)$, respectively.

In order to utilize the errors calculated by using (9) to determine the faulted section, the definition of the bus impedance matrix is used: An element $Z_{\text{bus}}(I, J)$ is defined as the voltage produced at node I due to a unit current injected at node J, with all other current injections being zero. Mathematically, for an N-dimension Z_{bus} [30]

$$Z_{\text{bus}}(I, J) = \frac{V_I}{I_J}\Big|_{I_k=0,\ K=1 \ldots N,\ K \neq J}. \tag{12}$$

It is obvious from this definition that the error index created as described in (9) will be the smallest for the bus closest to the actual fault location. For example, if the fault is in section $B(6) - B(7)$, as shown in Fig. 4, $\text{error}(6)$ and $\text{error}(7)$ will be the smallest, though one can be greater than the other depending on the fault being closer to $B(6)$ or $B(7)$. Thus, the faulted section can be identified as the section between buses that have the two smallest error indices. The flowchart depicting this procedure is shown in Fig. 5. There is, however, a chance of false

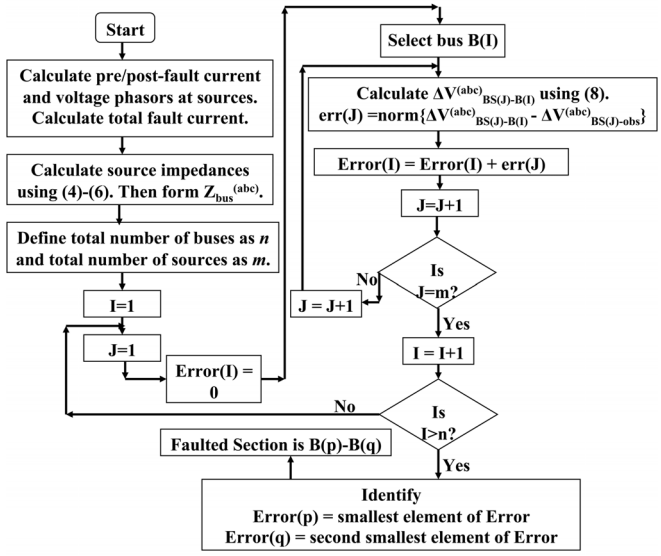

Fig. 5. Algorithm to identify the faulted section.

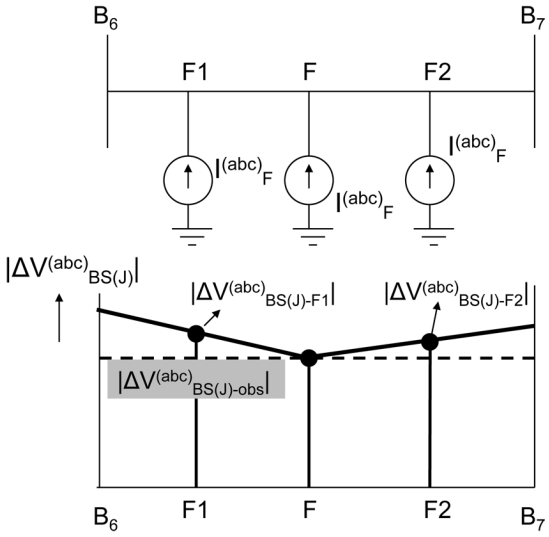

Fig. 6. Pictorial representation of the rationale behind the fault location.

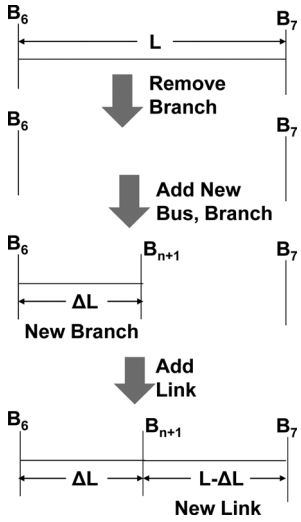

Fig. 7. Procedure to modify $Z_{\rm bus}$ to create a new bus.

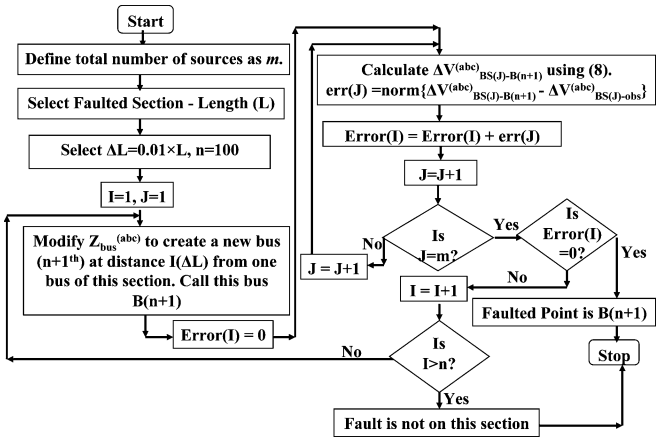

Fig. 8. Algorithm to locate the fault on a given section.

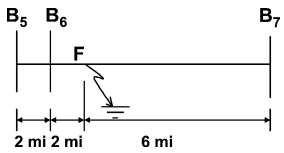

Fig. 9. Case for error in the section-identification algorithm.

estimation of the faulted section in certain cases with this procedure. This will be addressed after discussing the second part of the algorithm.

The second part of the algorithm extends the same rationale as used in the first part to locate the fault exactly on the faulted section identified in the first part. Fig. 6 shows the reasoning behind the method pictorially, assuming that section $B6-B7$ is faulted. The actual fault is at F. If the fault current is injected at F, the calculated magnitude of the voltage change at source J, $\left|\Delta V^{(abc)}_{BS(J)-F}\right|$ will be the same as the observed magnitude of the voltage change at source J, $\left|\Delta V^{(abc)}_{BS(J)-obs}\right|$ (i.e., the error calculated by (9) will be zero). However, from the geometry of the network in Fig. 4 and the properties described by (8) and (12), it is easy to see that if the fault current is injected at any other point between $B6$ and $B7$ (such as $F1$, $F2$), the errors calculated by using (9) will be greater than zero.

The fault locating algorithm starts by modifying $Z^{(abc)}_{\rm bus}$ to create a new bus at a small distance ΔL from $B6$. This is done by using the $Z_{\rm bus}$ building algorithm [30], [31] to remove section $B6-B7$, then adding a branch of length ΔL to bus $B6$ (thus creating the new bus) and then adding a link between the new bus and $B7$. This is illustrated in Fig. 7. The actual fault current is assumed to be injected at the new bus and the change in the voltages at terminals $BS(j)$ $(j=1,2\ldots m)$, $\Delta V^{(abc)}_{BS(j)-(NewBus)}$ are calculated by using (8). The error index for this new bus is then calculated by using (9). This procedure is repeated by progressively choosing the new bus farther away from $B6$. The fault point is identified when the error index has zero value. Fig. 8 shows the flowchart describing this algorithm.

Now, a note about the section-identification algorithm is in order. There is a chance of a wrong section being identified. A typical case is shown in Fig. 9. Since the buses closest to the actual fault are $B5$ and $B6$, $\text{error}(6) < \text{error}(5) < \text{error}(7)$. Therefore, the algorithm will identify $B5-B6$ as the faulted section. However, the fault is in section $B6-B7$. This confusion can be easily cleared by tracing the actual fault point on both sections according to the algorithm in Fig. 8. Fig. 10 shows the voltage profile similar to the one shown in Fig. 6 for both sections. It is easy to observe that the difference $\Delta V^{(abc)}_{BS(j)-(NewBus)} - \Delta V^{(abc)}_{BS(j)-obs}$ will never be zero for section $B5-B6$, but will be zero at the fault point F on section $B6-B7$. Thus, it is recommended that more than one *likely* section should be identified by using the section-identification algorithm, and the fault-location algorithm should be run on them one by one until a point corresponding to zero-error is found in order to single out the actually faulted section as well as the fault point. The four most likely sections were identified and were found to be sufficient for the simulation results described in Section III.

The method just discussed can be formulated with different numbers of DG units and can accommodate any change in the topology of the distribution system. These changes, such as the

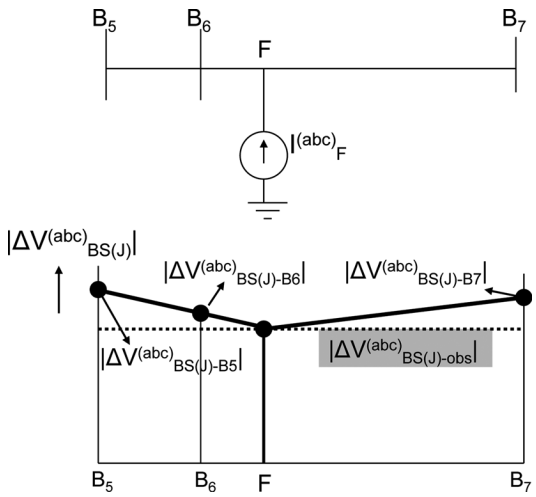

Fig. 10. Method to remove error in the section-identification algorithm.

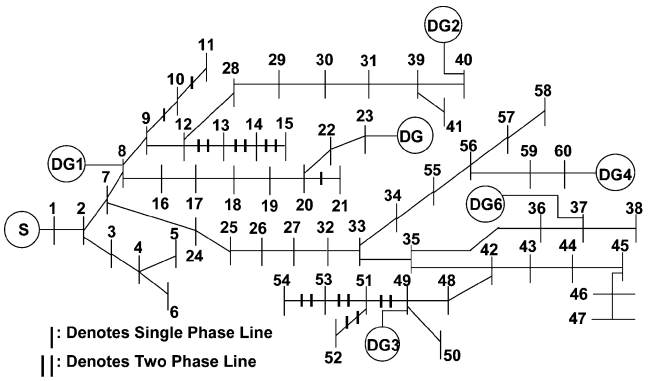

Line	From	To	Line	From	To	Line	From	To
1	1	2	21	20	22	41	35	42
2	2	3	22	22	23	42	42	43
3	3	4	23	7	24	43	43	44
4	4	5	24	24	25	44	44	45
5	4	6	25	25	26	45	45	46
6	2	7	26	26	27	46	46	47
7	7	8	27	12	28	47	42	48
8	8	9	28	28	29	48	48	49
9	9	10	29	29	30	49	49	50
10	10	11	30	30	31	50	49	51
11	9	12	31	27	32	51	51	52
12	12	13	32	32	33	52	51	53
13	13	14	33	33	34	53	53	54
14	14	15	34	33	35	54	34	55
15	8	16	35	35	36	55	55	56
16	16	17	36	36	37	56	56	57
17	17	18	37	37	38	57	57	58
18	18	19	38	31	39	58	56	59
19	19	20	39	39	40	59	59	60
20	20	21	40	39	41			

DG1: 0.4 MVA, DG2: 0.15 MVA, DG3: 0.45 MVA, DG4: 0.017 MVA, DG5: 0.1 MVA, DG6: 0.1MVA

Fig. 11. Distribution system simulated for testing.

connection/disconnection of lines, DG units, or capcitor banks, will be reflected as a modification of $Z_{\rm bus}^{(abc)}$.

III. Simulation Results

The fault-location scheme described in Section II-B was tested on an actual 12.47-kV distribution system from a utility located in the southeastern region in the U.S. The simulations were performed using PSCAD/EMTDC. The system topology is shown in Fig. 11 and load details can be found in [28]. The total load on the system is 2.5 MVA. Simulations were run with four, five, and six solidly grounded DG units connected to the system at randomly selected buses. The capacities of the DG units are shown in Fig. 11. The total capacity of all units form 49% of the total load on the system. Each DG unit was modeled as a source behind an impedance. Each line section was modeled as a "coupled Pi Model" in PSCAD/EMTDC, which is essentially a phase impedance matrix. This model captures any unbalance that may exist and the capacitance to ground. Since a cable and an overhead line can be modeled with this matrix, this method is applicable to any system with a combination of underground and overhead lines. The loads were modeled as constant-power loads. This means that they are not included in the $Z_{\rm bus}$. The loads will decide the prefault conditions of the simulated system. The capacitor bank is modeled as a constant-impedance load and, hence, is included in the $Z_{\rm bus}$.

The voltage and current waveforms were recorded at the substation source and at the output terminals of each DG. These waveforms were transferred to MATLAB and converted to synchronized phasors before and after the fault using full-cycle discrete Fourier transform (DFT). The sampling rate was chosen to be 48 kHz to remove any aliasing effect on DFT [34], since no analog antialiasing filter can be used in this digital-domain simulation. The data were then downsampled to 6 kHz for phasor calculations. These phasor values were used to calculate the source impedances for the substation source and for the DG units by using (4)–(6). These calculated values were used to build $Z_{\rm bus}^{(abc)}$. This ensured that $Z_{\rm bus}^{(abc)}$ modeled the system exactly at the time of fault (i.e., it was updated and accurate).

The phasors were processed with the algorithms shown in Figs. 5 and 8, implemented in MATLAB. The algorithm in Fig. 5 resulted in the identification of probable faulted sections, and the implementation of the algorithm in Fig. 8 on these probable sections resulted in the identification of the actual faulted section as well as the fault location on that section. At least one fault was simulated on each line. The fault type, fault resistance, and fault location were varied to cover all practical scenarios. The fault resistance for faults involving ground—line to ground and two line to ground—varied from 1 to 50 Ω. The fault resistance for three-phase faults and line-to-line faults varied from 1 to 5 Ω. These values are based on the arc resistance values quoted in [14]. For some of the simulations, two to three lines were removed and the $Z_{\rm bus}^{(abc)}$ was modified accordingly. The accuracy of the fault location was defined as

$$\%\text{Error} = \frac{\text{Actual Fault Location-Calculated Fault Location}\times 100}{\text{Length of Faulted Line Section}}. \tag{13}$$

Table I shows the simulation results. The fault distance was chosen to be 5%, 50%, and 95% from the sending end of each line section, and the fault resistance was varied within the practical bounds depending on the type of fault [14].

The results shown in Table I include results with four DG units (at buses 8, 40, 49, 60); five DG units (additional DG unit at bus 23); and six DG units (additional DG unit at bus 37). For the cases where the faulted line section could not be identified correctly, or where the error in fault location was more than 5%, the simulations were run with additional DG units to see if the problems could be overcome. The summary of the success rate is given in Table II. It is clear that even for low DG penetration

TABLE I
SIMULATION RESULTS

Line	*Fault Type*	*Fault Resistance (Ohms)*	*Fault Dist. (%)*	*Probable Lines*	*Final Line*			*% Error*		
					4 DG	5 DG	6 DG	4 DG	5 DG	6 DG
1	BG	50	50	1	1			0		
2	AG	10	5	2	2			0		
3	LLL	1	50	3	3			0		
3	LLL	5	95	4, 5, 3	4			0		
4	BC	1	5	4	4			0		
5	LLL	10	50	5	5			2		
6	ACG	1	95	6	6			0		
6	ACG	25	95	6	6			0		
7	CG	5	5	1, 4, 5, 7	7			0		
8	AG	10	50	20, 21, 22, 23	??	8*		0^{+}	0	
9-1-ph	AG	5	95	10, 9	9			0		
10-1ph	AG	25	5	10	10			4	4	4
11	LLL	1	50	11	11			0		
12-2ph	AB	5	95	13, 12	12			0		
13-2ph	AG	10	5	14, 13	13			0		
14-2ph	BG	50	50	14	14			0		
15	ABG	5	95	16, 17, 15	15			0		
16	BC	1	5	16	16			0		
17	CG	20	50	18, 17	17			0		
18	LLL	2	95	18	18			8	0	
19	BCG	5	5	18, 19	19			0		
20-1ph	AG	10	50	20	20			2		
21	BG	5	95	22, 21	21			0		
22	CA	1	5	22	22			0		
23	CAG	10	50	23	23			0		
24	LLL	1	95	24	24			0		
25	CG	5	5	6, 24, 25	25			0		
26	AG	10	50	26	26			0		
27	ABG	5	95	12, 13, 14, 27	27			0		
28	BG	50	5	13, 14, 27, 28	28			0		
29	AB	1	50	29	29			0		
30	LLL	5	95	38, 30	30			0		
31	CG	10	5	26, 31	31			0		
32	BC	5	50	32	32			0		
33	BCG	10	95	33	33			0		
34	LLL	1	5	34	34			0		
35	AG	1	50	35	35			0		
36	CA	3	95	36	36			0		
37-1ph	AG	25	5	37	37			0		
38	AB	5	50	40, 38	38			0		
39	LLL	1	95	38,39,40	39			0		
40	BG	10	5	40	40			0		
41	CG	5	50	46, 44, 45	??	??	41**	0^{+}	0^{+}	0
42	AB	5	95	42	42			0		
43	BCG	1	5	43	43			2		
44	LLL	1	50	44	44			1		
45	AG	15	95	45	45			0		
46	BC	2	5	46	46			1		
47	CAG	5	50	42, 47	47			0		
48	LLL	1	95	47, 49, 48	48			0		
49	BG	25	5	49	49			0		
50-2ph	AB	4	50	49, 50	50			0		
51-2ph	ABG	6	95	51	51			0		
52-2ph	AG	10	5	51, 53, 52	52			0		
53-2ph	BG	50	50	53	53			0		
54	LLL	3	95	55, 54	54			0		
55	CG	1	5	55	55			0		
56	BCG	7	50	56	56			0		
57	BC	3	95	57	57			0		
58	LLL	5	5	55, 56, 58	58			0		
59	AG	8	50	59	59			0		

* Sections initially identified are 10, 9, 8. ** Sections initially identified are 34, 45, 46, 41. $^{+}$ This result corresponds to running the algorithm on a known faulted section.

(4 DG–6.7%) gives excellent results. Higher DG penetration yields even better results. This is not surprising since more measurements are available with more DG units, which makes the algorithm more robust. It is worth mentioning here that six DG units in a 60-bus system constitute only 10% penetration of DG. Even for this relatively low penetration, the proposed method provides 100% success. Since the method is designed for high DG penetration, it can be claimed that it is very successful. It

TABLE II
SUMMARY OF THE SIMULATION RESULTS

Success Rate / Cases	*Correct Line Identification (% of Simulated Cases)*	*Error in Fault Location $\leq$ 5% (% of Simulated Cases)*
4 DG	96.72	98.36
5 DG	98.36	100
6 DG	100	100

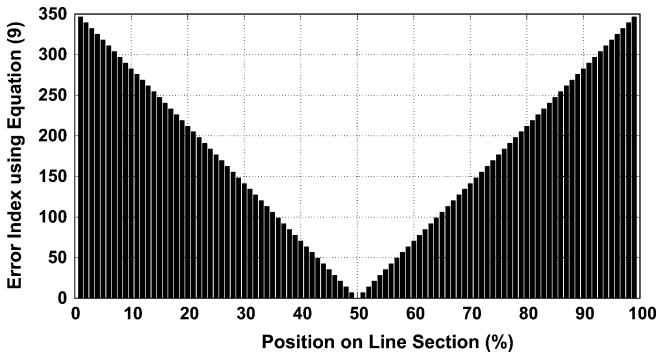

Fig. 12. Fault-location results from the implementation of the algorithm in Fig. 8 on line 32 for a BC fault in the middle of the line.

should also be noted that due to the way this method is formulated, it has no problem locating faults on sections forming radial forks. For example, faults on sections 4–5 and 4–6 were clearly distinguished and located.

Fig. 12 shows the typical profile obtained as a result of implementation of the fault-location algorithm described through the flowchart in Fig. 8. It can be seen that the error index is zero at the fault point, which is in the middle of the line for the case depicted. Almost all of the cases simulated gave just one zero value at the faulted point. Only a few cases where the error listed is more than zero in Table I gave zero errors for locations very close to the actual fault location. This may be ascribed to round-off errors in DFT and other calculations.

IV. CONCLUSION

It has been shown through this research that the detection of the faulted section and location of the fault on the faulted section are unresolved issues for distribution systems with significant penetration of DG. These issues will potentially impact the operation of distribution systems in the near future. A method to resolve these issues is proposed in this paper. The method uses measurement techniques that are available in the market today. The method is based on sound theoretical footing and is validated with extensive simulation results on a 60-bus distribution system. The simulation results indicate that the proposed method gives very satisfactory results even with relatively lower DG penetration. Correct line identification was achieved in 96.72% of the simulated cases and accurate fault location was achieved in 98.4% of the simulated cases even with a very low DG penetration of 6.7%. Higher DG penetration makes the method even more robust. With 10% DG penetration, 100% success was achieved. The method is immune to changes in the system topology, including addition/disconnection of the DG units, fault location, and fault resistance.

REFERENCES

[1] H. L. Willis and W. G. Scott, *Distributed Power Generation Planning and Evaluation*. New York: Marcel Dekker, 2000.
[2] C. Smoots and P. Coie, "Overview of state and federal incentives for the use of distributed generation," *Cogen. Distrib. Gen. J.*, vol. 21, pp. 7–59, 2006.
[3] T. Ackermann, G. Andersson, and L. Soder, "Distributed generation: A definition," *Elect. Power Syst. Res.*, vol. 57, pp. 195–204, 2001.
[4] D. Nichols, J. Stevens, R. Lasseter, J. Eto, and H. Vollkommer, "Validation of the CERTS microgrid concept the CEC/CERTS microgrid testbed," presented at the IEEE Power Eng. Soc. Gen. Meeting, Montreal, QC, Canada, 2006.
[5] "Distribution line protection practices: Industry survey analysis," *IEEE Trans. Power App. Syst.*, vol. PAS-102, no. 10, pp. 3279–3287, Oct. 1983.
[6] P. M. Anderson, *Power System Protection*. New York: IEEE Press/ McGraw-Hill, 1999.
[7] N. Hadjsaid, J. Canard, and F. Dumas, "Dispersed generation impact on distribution networks," *IEEE Comput. Appl. Power*, vol. 12, no. 2, pp. 22–28, Apr. 1999.
[8] A. A. Girgis and S. M. Brahma, "Effect of distributed generation on protective device coordination in distribution system," in *Proc. Large Engineering Systems Conf. Power Engineering Conf.*, Canada, 2001, pp. 115–119.
[9] S. M. Brahma and A. A. Girgis, "Distribution system protective device coordination in presence of distributed generation," *Int. J. Power Energy Syst.*, vol. 24–1, pp. 32–37, Jan. 2004.
[10] S. M. Brahma and A. A. Girgis, "Microprocessor-based reclosing to coordinate fuse and recloser in a system with high penetration of distributed generation," in *Proc. IEEE Power Eng. Soc. Winter Meeting*, 2002, vol. 1, pp. 453–458.
[11] S. M. Brahma and A. A. Girgis, "Effect of fault resistance on the coordination of a microprocessor-based recloser with a fuse in the presence of distributed generation," presented at the 9th Int. Middle-East Power Conf., Shebin El-Kom, Egypt, Dec. 2003.
[12] R. Dugan and T. McDermott, "Distributed generation," *IEEE Ind. Appl. Mag.*, vol. 8, no. 2, pp. 19–25, Mar./Apr. 2002.
[13] Power System Relaying Committee, Impact of distributed resources on distribution relay protection. [Online]. Available: http://www.pes-psrc.org/
[14] J. L. Blackburn, *Protective Relaying Principles and Applications*. New York: Marcel Dekker, 1998.
[15] Y. Lu, L. Hua, J. Wu, G. Wu, and G. Xu, "A study on effect of dispersed generator capacity on power system protection," presented at the IEEE Power Eng. Soc. Gen. Meeting, Tampa, FL, Jun. 2007.
[16] Z. Xiangjun, K. Li, W. Chan, and S. Sheng, "Multi-agents based protection for distributed generation systems," in , *Proc. IEEE Int. Conf. Electric Utility Deregulation, Restructuring and Power Technologies*, Apr. 2004, vol. 1, pp. 393–397.
[17] S. Javadian, A. Nasrabadi, M.-R. Haghifam, and J. Rezvantalab, "Determining fault's type and accurate location in distribution systems with dg using mlp neural networks," in *Proc. Int. Conf. Clean Electrical Power*, Jun. 2009, pp. 284–289.
[18] T. El-Fouly and C. Abbey, "On the compatibility of fault location approaches and distributed generation," presented at the CIGRE/IEEE Power Eng. Soc. Joint Symp. Integration of Wide-Scale Renewable Resources Into the Power Delivery System, Calgary, AB, Canada, Jul. 2009.
[19] J. Marvik, A. Petterteig, and H. Hoidalen, "Analysis of fault detection and location in medium voltage radial networks with distributed generation," *Proc. IEEE Power Tech Lausanne*, pp. 1191–1196, Jul. 2007.
[20] Z. Guo-fang and L. Yu-ping, "A fault location algorithm for urban distribution network with DG," in *Proc. 3rd Int. Conf. Electric Utility Deregulation and Restructuring and Power Technologies*, Apr. 2008, pp. 2615–2619.

[21] Z. Guo-fang and L. Yu-ping, "Development of fault location algorithm for distribution networks with DG," in *Proc. IEEE Int. Conf. Sustainable Energy Technologies*, Nov. 2008, pp. 164–168.
[22] S. Javadian, M. Haghifam, and N. Rezaei, "A fault location and protection scheme for distribution systems in presence of dg using mlp neural networks," in *Proc. IEEE Power Energy Soc. Gen. Meeting*, Jul. 2009, pp. 1–8.
[23] V. Calderaro, A. Piccolo, V. Galdi, and P. Siano, "Identifying fault location in distribution systems with high distributed generation penetration," *Proc. AFRICON*, pp. 1–6, Sep. 2009.
[24] Y. Chao, Z. Xiangjun, and X. Yunfeng, "Improved algorithm for fault location in distribution network with distributed generations," in *Proc. Int. Conf. Intelligent Computation Technology and Automation*, Oct. 2008, vol. 2, pp. 893–896.
[25] A. Bretas and R. Salim, "Fault location in unbalanced DG systems using the positive sequence apparent impedance," in *Proc. IEEE/Power Eng. Soc. Transmission Distribution Conf. Expo.: Latin America*, Aug. 2006, pp. 1–6.
[26] D. Johnsonbaugh and A. Girgis, "Fault location for distribution systems with distributed generation using a modified three phase method," presented at the Power Systems Conf. Distributed Generation, Advanced Metering and Communication, Clemson, SC, Mar. 2004.
[27] A. Girgis, C. Fallon, and D. Lubkeman, "A fault location technique for rural distribution feeders," *IEEE Trans. Ind. Appl.*, vol. 29, no. 6, pp. 1170–1175, Nov. 1993.
[28] S. M. Brahma and A. A. Girgis, "Development of adaptive protection scheme for distribution systems with high penetration of distributed generation," *IEEE Trans. Power Del.*, vol. 19, no. 1, pp. 56–63, Jan. 2004.
[29] P. Barker and R. W. de Mello, "Determining the impact of distributed generation on power systems: Part 1—Radial power systems," in *Proc. IEEE Power Eng. Soc. Summer Power Meeting*, 2000, pp. 1645–1658.
[30] J. Grainger and W. Stevenson , Jr, *Power System Analysis*. New York: McGraw-Hill, 1994.
[31] E. Makram and A. Girgis, "A generalized computer technique for the development of three-phase impedance matrix for unbalanced power system," *Elect. Power Syst. Res.*, vol. 15, pp. 41–50, 1988.
[32] E. Makram, A. Bou-Rabee, and A. Girgis, "Three phase modelling of unbalanced distribution systems during open conductor and/or shunt fault conditions using bus impedance matrix," *Elect. Power Syst. Res.*, vol. 13, pp. 173–183, 1987.
[33] J.-A. Jiang, Y.-H. Lin, J.-Z. Yang, T.-M. Too, and C.-W. Liu, "An adaptive PMU based fault location/location technique for transmission lines PART II: PMU implementation and performance evaluation," *IEEE Trans. Power Del.*, vol. 15, no. 4, pp. 1136–1146, Oct. 2000.
[34] S. M. Brahma, P. L. D. Leon, and R. G. Kavasseri, "Investigating the option of removing anti-aliasing filter from digital relays," *IEEE Trans. Power Del.*, vol. 24, no. 4, pp. 1864–1868, Oct. 2009.

Sukumar M. Brahma (M'04–SM'07) received the B.Eng. degree in electrical engineering from Lalbhai Dalpatbhai College of Engineering, Ahmedabad, India, in 1989, the M.Tech. degree in electrical engineering from the Indian Institute of Technology, Bombay, in 1997, and the Ph.D. degree in electrical engineering from Clemson University, Clemson, SC, in 2003.

From 2003 to 2007, he was Assistant Professor at Widener University, West Chester, PA. Currently, he is Assistant Professor and Associate Director of the Electric Utility Management Program (EUMP) at New Mexico State University, Las Cruces.

Prof. Brahma is a member of Sigma Xi, Past Chair of the IEEE Power Engineering Society's Life Long Learning Subcommittee, Chair of the Distribution System Analysis Subcommittee, and belongs to several working groups of the Power System Relaying Committee.